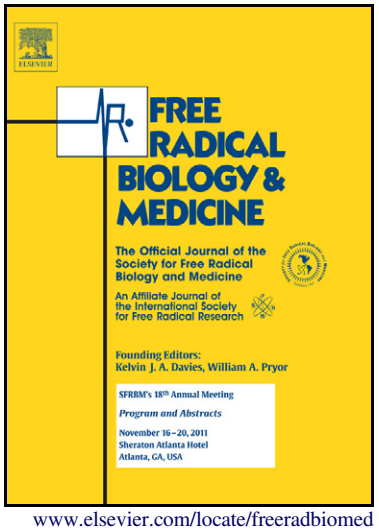

www.elsevier.com/locate/freeradbiomed

Membrane association of peroxiredoxin-2 in red cells is mediated by n-terminal cytoplasmic domain of band 3

Alessandro Matte, Mariarita Bertoldi, Narla Mohandas, Xiuli An, Antonella Bugatti, Anna Maria Brunati, Marco Rusnati, Elena Tibaldi, Angela Siciliano, Franco Turrini, Silverio Perrotta, Lucia De Franceschi

PII: S0891-5849(12)01774-1
DOI: http://dx.doi.org/10.1016/j.freeradbiomed.2012.10.543
Reference: FRB11357

To appear in: *Free Radical Biology and Medicine*

Cite this article as: Alessandro Matte, Mariarita Bertoldi, Narla Mohandas, Xiuli An, Antonella Bugatti, Anna Maria Brunati, Marco Rusnati, Elena Tibaldi, Angela Siciliano, Franco Turrini, Silverio Perrotta and Lucia De Franceschi, Membrane association of peroxiredoxin-2 in red cells is mediated by n-terminal cytoplasmic domain of band 3, *Free Radical Biology and Medicine,* http://dx.doi.org/10.1016/j.freeradbiomed.2012.10.543

MEMBRANE ASSOCIATION OF PEROXIREDOXIN-2 IN RED CELLS IS MEDIATED BY N-TERMINAL CYTOPLASMIC DOMAIN OF BAND 3

Alessandro Matte*, Mariarita Bertoldi°[2], Narla Mohandas^, Xiuli An^, Antonella Bugatti§, Anna Maria Brunati◆, Marco Rusnati§, Elena Tibaldi◆, Angela Siciliano*, Franco Turrini ‡, Silverio Perrotta[±], Lucia De Franceschi*[1]

* Department of Medicine,Section of Internal Medicine, University of Verona, AOUI-Policlinico GB Rossi, Verona; Italy

°Dept of Life and Reproduction Sciences, Section of Biochemistry, University of Verona, Verona; Italy;

^ New York Blood Center, New York, NY; USA

§ Sections of General Pathology and Immunology, Department of Biomedical Sciences and Biotechnology, University of Brescia, Brescia; Italy

◆Department of Biochemistry, University of Padova, Padova; Italy

‡ Dept of Biochemistry, University of Torino, Torino; Italy;

[±] Department of Pediatric, II University of Naples, Naples; Italy

Corresponding Authors

Lucia De Franceschi *[1] and Mariarita Bertoldi °[2]

* Dept. of Medicine, University of Verona; Policlinico GB Rossi, P.le L Scuro, 10

37134 Verona, Italy; FAX: +390458027473; phone: +390458124918; E-mail lucia.defranceschi@univr.it

° Dept. of Life and Reproduction Sciences, Section of Biochemistry, University of Verona, Verona, Italy; Section of Biochemistry, University of Verona, Strada Le Grazie 8, 37134 Verona, Italy; FAX: +390458027170; phone: +390458027671; E-mail: mita.bertoldi@univr.it

ABSTRACT

Band-3 (B3), the anion transporter is an integral membrane protein that plays a key structural role by anchoring the plasma membrane to the spectrin-based membrane skeleton in the red cell. In addition, it also plays a critical role in the assembly of glycolytic enzymes to regulate red cell metabolism. However, its ability to recruit proteins that can prevent membrane oxidation has not been previously explored. In the present study, using a variety of experimental approaches including cross-linking studies, fluorescence and dichroic measurements, surface-plasmon-resonance analysis, and proteolytic digestion assays, we document that the anti-oxidant protein, Peroxiredoxin-2 (PRDX2), the third most abundant cytoplasmic protein in RBCs, interacts with the cytoplasmic domain of B3. The surface electrostatic potential analysis and stoichiometry measurements revealed that the N-terminal peptide of B3 is involved in interaction. PRDX2 underwent a conformational change upon its binding to B3 without losing its peroxidase activity. Hemichrome formation induced by phenylhydrazine (PHZ) of RBCs prevented membrane association of PRDX2 implying over lapping binding sites. Documentation of the absence of binding of PRDX2 to B3 Neapolis red cell membranes in which the initial N-terminal 11 amino acids are deleted, enabled us to conclude that PRDX2 binds to the N-terminal cytoplasmic domain of B3 and that the first 11 amino acid of this domain are crucial for PRDX2 membrane-association in intact RBCs. These findings imply yet another important role for B3 in regulating red cell membrane function.

Key words: peroxiredoxin-2, band 3, red cell membrane

INTRODUCTION

Human red cells have been extensively studied and a general model for the structural organization of its membrane organization has been developed [1]. Macromolecular complexes of integral proteins embedded in the bilayer are anchored by linker proteins to a supramolecular structure designated as membrane skeleton. Band 3, the major integral membrane protein though its interaction with ankyrin links the bilayer to the spectrin-based skeletal protein network and plays a critical role in maintaining membrane cohesion [1]. Band 3 also plays a crucial role in membrane association of glycolytic enzymes and thereby regulate cell metabolism [2]. As it is also the major interacting partner for denaturated hemoglobin and hemichrome, it can also play

a role in bringing powerful oxidants in close proximity the membrane and to the multiprotein complexes [2, 3], which

can induce detrimental oxidant damage to red cell membrane. In red cells peroxiredoxin-2 (PRDX2) is the third most abundant cytoplasmic protein and is a typical 2-cysteine (Cys) peroxiredoxin [4-6]. PRDX2 acts as antioxidant for endogenously generated H_2O_2, but recent evidence suggests a cellular role of PRDX2 as molecular chaperone in various cell models [7]. In red cells, PRDX2 (formerly termed calpromotin) was initially characterized as a membrane-associated protein, whose reversible binding to the membrane was linked to regulation of the Ca^{2+}-activated K^+ channel (Gardos channel) *via* a still undefined mechanism [8-11]. In a mouse model for sickle cell disease characterized by abnormal activation of the Gardos channel, we have recently shown that the PRDX2 membrane association is modulated during hypoxia through an undefined mechanism [12]. The nature of association of PRDX2 to the red cell membrane is still unclear. Moore et al. using a PRDX2 affinity column prepared with purified protein from red cells found that only stomatin but not other integral membrane proteins such as band 3 or membrane skeletal protein such as α- or β-spectrin bound PRDX2 [9]. However, this earlier study had some limitations: (i) peroxidase assay of the purifed PRDX2 was not documented; (ii) monomeric PRDX2, with a molecular weight < 30,000 Da was used for binding studies [13], although the active forms of PRDX2 are higher oligomers such as decamers.

To overcome these limitations, in the present study we used native recombinant active PRDX2 to indentify its binding partners in the red cell membrane and documented the cytoplasmic domain of B3 binds PRDX2. These findings enabled us to document a potentially important role for B3 in preventing membrane oxidant damage by recruiting proteins that can mitigate oxidant damage.

MATERIALS AND METHODS

Drugs and Chemicals. Details are reported in Supplementary Materials and Methods.

Red cell membrane ghost preparation. Blood was drawn from healthy volunteers and from a subject homozygous for band 3 Neapolis mutation [14]; according to the guidelines established by the local Ethic Committee for human subject studies. Written informed consent to the study was obtained from all the participants. Blood was centrifuged at 3000 g for 5 min at 4°C to remove plasma, passed through cotton to remove white cells, and washed three times with

choline wash solution (CWS: 155 mM choline, 1 mM $MgCl_2$, 10 mM Tris-MOPS pH 7.4 at 4 °C, 290-300 mOsm) [15, 16]. Packed red cells were lysed in phosphate lysis buffer (PLB: 5 mM Na_2HPO_4 pH 8.0, added of a protease inhibitor cocktail tablet, 3 mM benzamidine, 1 mM Na_3VO_4 final concentration) and washed in PLB 5 times to obtain almost white ghosts [17, 18]. Whenever PRDX2 was evaluated in one-dimensional (1D) SDS-PAGE analysis, 100 mM of NEM was added to the PLB to avoid possible artifacts due to PRDX2 oxidation after cell lysis [18]. Red cell total lysates were prepared lysing packed RBCs in E-Buffer 4X (EB-4X, 200 mM Tris pH 7.4, 400 mM NaCl, 20 mM EDTA pH 7.4, 4% Triton X-100, protease inhibitor cocktail tablet (Roche), 3 mM benzamidine and 1 mM Na_3VO_4 final concentration) and left rotating for 1 hr at 4 °C to complete lysis and protein solubilization [18-20].

Treatment of red cells with different oxidative agents and crossing- experiments. Red cells underwent to treatment with two different oxidative agents diamide (2 mM) and phenylhydrazine (PHZ 100 μM) based on preliminary dose response studies and previously reported data in both human and mouse erythrocytes [18, 21, 22]. Whenever indicated Na_3VO_4 (0.1 mM) was present in the incubation media [21]. Details are reported in Supplementary Materials and Methods.

Immunoblot analysis of red cell membranes. For mono-dimensional electrophoresis proteins from ghosts and cytosol fraction were carried out as previously described by Matte et al [18]. Details are reported in Supplementary Materials and Methods.

KI-IOV generation and PRDX2 label transfer study. KI-stripped inside-out erythrocyte membrane vesicles (KI-IOV) were prepared from red cell ghosts as previously reported by Anong et al. [23]. Details are reported in Supplementary Materials and Methods.

cdb3 preparation. cdb3 and phospho-cdb3 was prepared as previously described [24]. Details are reported in Supplementary Materials and Methods.

Fluorescence measurements. PRDX2 (4 μM, 0.09 mg/ml)) intrinsic fluorescence spectrum was measured by exciting the enzyme at 295 nm, at which tryptophan residues have their absorbance maximum, and recording spectra in the interval from 300 to 500 nm with a Jasco FP750 spectrofluorimeter in 50 mM sodium phosphate buffer, 0.1 M NaCl, pH 7.4, or in 50 mM Hepes, pH 7.4 at 25°C. Experimental details are reported in Supplementary Materials and Methods.

Far and near UV-visible circular dichroism measurements. Circular dichroism (CD) measurements were performed as reported in Supplementary Materials and Methods.

Limited tryptic proteolysis. PRDX2 sample (0.5 mg protein/ml, corresponding to 22.6 μM) or PRDX2 (0.4 mg/ml, 20 μM) bound to cdb3 (0.1 mg/ml) were incubated at 25 °C in 50 mM HEPES, pH 7.4 with trypsin (1:50, w:w). At various times (0.5, 1, 2, 5, 10, 15, 30 min) after the addition of trypsin, aliquots were withdrawn, heated at 100°C for 3 min, diluted in sample buffer for SDS-PAGE and analyzed electrophoretically.

Peroxidase activity. PRDX2 activity was measured as previously reported [25].

Real time surface plasmon resonance (SPR) analyses of PRDX2/cdb3 interaction. SPR measurements were performed on a BIAcore X instrument (GE-Healthcare, Milwaukee, WI). Details are reported in Supplementary Materials and Methods [26]. **Electrostatic potential surface calculation.** The 3D coordinates of erythrocyte PRDX2 were downloaded from the Protein Data Bank (1QMV, [6]) while the 11 aa N-terminal peptide of cdb3 was built using SPDB-Viewer. Electrostatic calculations on the protein/peptide were carried out by solving the nonlinear Poisson-Boltzmann equation, one of the most popular continuum models for describing electrostatic interactions between molecular solutes in salty, aqueous media. Adaptive Poisson-Boltzmann Solver was used to this purpose [27] with a protein and solvent dielectric constants of 2-4 and 80, respectively.

Stoichiometry experiments. The molar ratio of the complex between PRDX2 and cdb3 was measured from the staining intensities of the proteins in the pellet by SDS-PAGE. Experimental details are reported in Supplemental Materials and Methods.

Immunofluorescence assay. Immunofluorescence analysis for PRDX2 was carried out as we previously described by [18].

Statistical analysis. The 2-way ANOVA algorithm for repeated measures between treatments was used for data analysis. Differences with $p<0.05$ were considered significant.

RESULTS

PRDX2 translocates to the membrane in response to oxidative stress and binds to 3 the cytoplasmic domain of band 3.

We first evaluated membrane association of PRDX2 in human red cells in response to different oxidative stress induced by either PHZ or diamide (Fig. 1A, Fig. 1SA, 1SB). Similar to our earlier finding with mouse red cells, PRDX2 membrane association was undetectable in PHZ treated human red cells, while membrane association of PRDX2 was significantly increased in diamide treated cells, it was undetectable in PHZ treated human red cells [18]. Since PRDX2 dimerization occurs in response to oxidative stress [4], we evaluated if this differential membrane association of PRDX2 following oxidative stress is the consequence of different effects of diamide and PHZ on PRDX2 dimerization.

PRDX2 dimers were found only in diamide treated red cells (Fig. 1B, 1SC, 1SD) but not in PHZ treated red cells. Thus the differential membrane association is possibly related to the different forms of oxidative damage induced by PHZ and diamide as the former generates free radical species resulting in the production of hemichromes that bind to the membrane, while the latter is a cysteine-reacting agent. In fact, the amount of hemichromes bound to the membrane was significantly increased in PHZ treated red cells compared to either control or diamide treated red cells (Fig. 1SE). We have previously shown competitive membrane association between hemichromes and PRDX2 in mouse red cells [18] and based on the reported association of denatured hemoglobin to the cytoplasmic domain of band 3 [28], we hypothesized that N-terminal band 3 cytoplasmic domain may represent a binding site for PRDX2 on red cell membrane, which is masked by hemichrome binding to band 3 in PHZ treated red cells.

The N-terminal band 3 cytoplasmic domain plays a key role in dynamic recruitment of various proteins to the red cell membrane. Different stimuli such as the state of tyrosine phosphorylation state or deoxygenation can modulate the ability of these proteins to bind band 3 [2, 3]. We therefore evaluated whether membrane association of PRDX2 in red cell is affected following treatment with Na-vanadate, a phosphatase(s) inhibitor [29, 30] or by binding of deoxyhemoglobin to bind to band 3 following deoxygenation [31]. Two Tyr-residues (Tyr 8 and 21) present in N-terminal domain of band 3 are targets of Syk-Lyn tyrosine kinase pathway [30]. We first evaluated the phosphorylation of Tyr 8 of band 3 in red cells treated with oxidants. While no increase in phosphorylation of Tyr 8 was noted in PHZ treated red cells compared to untreated control erythrocytes (Fig. 1A, Fig. 1SA, 1SB), a marked increase in phosphorylation of Tyr 8 was noted following treatment with diamide (Fig. 1A). In the presence of Na-vanadate, we found increased extents of phosphorylation of Tyr-8 of band 3 in control red cells as well as in PHZ treated red cells and in diamide treated red cells (Fig. 1A, Fig. 1SA, 1SB). The combined

treatment with Na-vanadate and diamide produced highest levels of phosphorylation of Tyr-8 on band 3 in agreement with previous reports [29, 30].

As these studies involved exposing intact red cells to oxidative agents it is difficult to discriminate if the observed effects on membrane association of PRDX2 are the result of membrane modifications or modification of PRDX2 or both. In order to address this issue, we compared the ability of control membranes and control membranes pre-treated with PHZ, diamide and Na-vanadate to bind PRDX2 in the cytoplasmic fraction of control RBCs. We did not observe PRDX2 membrane translocation in PHZ treated red cell membrane; whereas, PRDX2 was associated to the membrane in control, diamide and Na-vanadate treated red cell membrane similarly to that observed in intact erythrocytes (Fig. 1C, 2SA, 2SB). In order to validate the hypothesis that band 3 occupancy by hemichromes might mask PRDX2 binding site, we treated isolated red cell membrane with either PHZ or diamide to induce oxidative damage in the absence of hemoglobin to prevent membrane association of hemichromes or other heme compounds. As shown in Fig. 1C, the native PRDX2 was able to translocate to the membrane in both PHZ and diamide treated red cell membrane, suggesting that membrane association of hemichromes prevents PRDX2 binding to red cell membrane.

We next evaluated the effect of deoxygenation on the ability of PRDX2 to bind to red cell membrane. As shown in Fig. 1D, PRDX2 membrane association was increased following red cell deoxygenation. Taken together these data suggest that cytoplasmic domain of band 3 is likely the binding site for PRDX2 on red cell membrane.

PRDX2 interacts with the N-terminal domain of band 3.

To further validate the binding of PRDX2 to band 3 on the red cell membrane, we performed cross-linking studies, using recombinant PRDX2 [25] labeled with a photoactivatable cross-linking probe (sulfo-SBED). The labeled probe was incubated with KI-IOVs as previously described by Anong et al. [23]. Four bands on KI-IOVs with molecular weight of ~ 250 kDa, ~ 95 kDa and between 95 and 72 kDa (Fig. 2A) reacted with sulfo-SBED-PRDX2. Probing of these membranes with specific antibody against band 3 and α-,β-spectrin, whose molecular weights correspond to reacting proteins identified as well as mass spectrometric analysis of the corresponding bands confirmed their identities as α-,β-spectrin, band 3, band 4.1 and protein 4.2.

Since band 3 was identified as one of the major interacting partners of PRDX2, we carried out experiments with recombinant PRDX2 and the cytoplasmic N-terminal domain of band 3 (cdb3) using multiple biochemical approaches. As shown in Fig. 2B, tryptophan fluorescence of native recombinant PRDX2 (4 μM) (following excitation at 295 nm) showed an emission maximum at 338 nm [25] in 50 mM sodium phosphate buffer, 0.1 M NaCl, pH 7.4 or in 50 mM Hepes pH 7.4. The addition of cdb3 induced a significant quenching of this emission that drops from 271 to 218 a.u. when cdb3 was present in excess (Fig 2B). Analysis of changes in fluorescence emission as a function of cdb3 concentration yielded a hyperbolic curve whose fitting resulted in a equilibrium dissociation constant (Kd) of 34 ± 4 nM (inset Fig 2B). We also measured the affinity of PRDX2 with phosphorylated cdb3 by evaluating the quenching of intrinsic fluorescence and found no significant changes in equilibrium dissociation constant Kd = 57 ± 7 nM (data not shown). Thus, PRDX2 binds to either unphosphorylated or phosphorylated cdb3 with similar binding affinities.

To further validate that N-terminal band 3 indeed constitutes a docking site for PRDX2 we used the surface plasma resonance strategy with cdb3 immobilized on a BIAcore sensorchip. PRDX2 (900 nM) specifically bound to immobilized cdb3 but not to immobilized anti- N-terminal band 3 antibody surface (Fig. 2C, upper panel). Also, injection of increasing concentrations of PRDX2 (Fig. 2C, lower panel) over immobilized cdb3 enable the determination of the kinetic parameters of the cdb3/PRDX2 interaction, that occurs with a kinetic association rate (k_{on}) of 148 M^{-1} s^{-1} and a kinetic dissociation rate (k_{off}) equal to 9.76 x 10^{-6} s^{-1}, resulting in high affinity [dissociation constant (K_d) value equal to 66 nM. As internal control, under the same experimental conditions, immobilized cdb3 interacts with its specific antibody anti- N-terminal band 3 antibody with a K_d equal to 1.9 nM (Table 1), a value that is consistent with affinities reported in literature for the Ab/Ag interaction. Thus use of two different experimental approaches has enabled us to document a high affinity interaction between PRDX2-cdb3 in the nM range.

PRDX2 undergoes a conformational change upon binding to cdb3. In order to determine if changes in the conformation of cytoplasmic domain of band 3 occurs following its interaction with PRDX2, we carried out circular dichroism (CD) studies in the near UV-visible region. Near UV-visible circular dichroic (CD) spectrum of PRDX2 (20 μM, 0.44 mg/ml) in 50 mM Hepes, pH 7.4 was characterized by a broad signal in the 270-300 nm region due to aromatic amino acid side chains (Fig. 2D). Addition of 0.1 mg/ml (i.e. 2.3 μM) cdb3 resulted in a time-dependent splitting of CD spectra characterized by a decrease at 275 nm and a concomitant formation of a peak at 284 with maximal changes seen between 15-30 min (Fig. 2D). These observed spectral

changes suggest a conformational change in PRDX2 following its interaction of with cdb3. Further validation of such a conformational change was obtained from limited tryptic digestion studies PRDX2 in the presence and absence of cdb3. A preliminary search with the PeptideCutter tool on the Bioinformatic Resources Portal Expasy (http://www.expasy.ch/tools) indicated 22 putative trypsin sites in PRDX2. PRDX2 (0.5 mg/ml) subjected to trypsin digestion (1:50, w:w) showed a time-dependent degradation that was almost complete in 5 minutes (Fig. 2SD). Addition of cdb3 (0.1 mg/ml) to PRDX2 (0.4 mg/ml) followed by 20-min incubation largely protected PRDX2 from trypsin cleavage and more than 80% of intact PRDX2 was present after 30 min of incubation (Fig. 2SE). Moreover, peroxidase activity of PRDX2 was fully conserved when it was bound to cdb3, thus excluding an active role of the catalytic cysteine residues in interaction.

The nature of the interaction of PRDX2 with cdb3 is electrostatic. Since it was previously reported that cdb3 is highly flexible and undergoes pH-dependent conformational changes ([32] and references therein), we studied the interaction of PRDX2 with cdb3 at pH 8.5 and pH 6.4. PRDX2 at concentration of 4 μM in 50 mM Hepes pH 8.5 was excited at 295 nm and emission at 338 nm was measured, Plotting the difference in emission at 338 nm as a function of cdb3 concentration yielded an hyperbolic curve and analysis of this different spectra yielded an equilibrium dissociation constant, Kd of 110 ± 7 nM, a value that is approx. 3-times higher than that measured at pH 7.4 (Fig. 3S). As either PRDX2 or cdb3 far UV CD spectra are not modified in this pH range (data not shown), we can excluded the potential contribution of major structural alterations of either of these two proteins for the observed alterations in binding affinity.

When we tried to perform the same fluorimetric analysis at pH 6.4 we noted turbidity of PRDX2 solution following addition of cdb3 thereby preventing the performance of any fluorescence spectral analysis. Such precipitation has been also described when cdb3 is added to a solution of hemichromes at low pH in a low ionic strength buffer [28]. It should be noted that when the pH of the PRDX2 solution was gradually increased, turbidity disappeared.

The stoichiometry of cdb3: PRDX2 complex is dimer to decamer.

In order to assess if the observed precipitation at pH 6.4 is the result of co-polymerization of interacting proteins, rather than a simple mass aggregation of denatured proteins, we mixed PRDX2 with different amounts of cdb3 (2:1 or 1:1) in 50 mM Hepes pH 6.4. If the event is driven by mass, the ratio of the proteins in the precipitate will be dependent upon their ratio in solution, whereas if it is the result of co-polymerization, the same molar ratio will be present in the

precipitate irrespective of their differing concentration in the incubation mixture. Using such an approach as previously outlined [28], we allowed the two incubation mixtures described above to equilibrate for 15 minutes and following centrifugation, separated the supernatants from the pellet, solubilized them in SDS sample buffer and run the aliquots by SDS-PAGE. As shown in Fig. 3A, P1 and P2 representing the pellets of the two different mixtures gave the same molar ratio: five PRDX2 monomers per one cdb3 monomer, implying that the functional decameric PRDX2 interacts with the functional dimeric cdb3. Thus, a defined stoichiometry drives the interaction of PRDX2 with cdb3, further validating the molecular specificity of this interaction.

Electrostatic potential surface calculation of PRDX2.

Given the differential behaviour of the mixtures composed by PRDX2 and cdb3 at different pH values, we argued if the interaction between the two proteins partly relies on their electrostatic surfaces and which is the structural motifs are involved in the interaction. Since the isoelectric point of PRDX2 as calculated by the Expasy Protein Parameters tool (http://www.expasy.ch/tools/) is 5.66, the protein should be mainly acidic at physiological pH. However, the observation that PRDX2 does not bind to anion-exchange resins at pH 7.5 (data not shown) along with the fact that it does not enter into the running gel in a native polyacrylamide gel electrophoresis (data not shown), led us to suppose that the surface should also present a pronounced basic character. When we perform a calculation of the electrostatic surface, it can be seen that the dimeric protein presents extensive basic surfaces. One is located as a string (Fig. 4SA), at the interface between the two monomers that are arranged in an antisymmetric fashion [6], while the other extends on one of the two flat faces of the dimer (Fig 4SB) on the opposite side of the crevices between the two monomers. In the decameric structure these basic electrostatic potential surfaces point towards the center of the five-dimeric thoroid structure (Fig. 3B), thus conferring a highly basic character to the hole in the center of the decameric ring. The first part of the N-terminus of band 3 (55 amino acids) serves as a critical organizing center for binding of several proteins [33-39]. In particular, the first 11-amino acids of the N-terminal peptide have a particularly pronounced acidic character (Fig. 4SC) and could be considered as a good candidate for binding to the center of the ring of decameric PRDX2.

The first 11-amino acid peptide of the N-terminal of band 3 is required for PRDX2 membrane association in vivo. To further demonstrate that the N-terminal cytoplasmic domain of band 3 is important for PRDX2 membrane association, we evaluated PRDX2 protein

distribution in red cells from a patient with mutation in the band 3 gene that results in the complete absence of the first 11 N-terminal amino acids of band 3 (band 3 Neapolis) [14]. In a previous study, we have shown that this mutated protein does not bind glycolytic enzymes and furthermore cannot undergo tyrosine phosphorylation [14]. As shown in Fig. 3, the association of PRDX2 to red cells membrane was assessed by two different methodological approaches. No PRDX2 could be detected in association with the red cell membrane of band 3 Neapolis patient, while it was detectable in controls. PRDX2 was present in cytosol fraction and in total red cell lysates from band 3 Neapolis patient (Fig. 4A). In agreement with immunoblot analysis, the confocal images showed PRDX2 as cytoplasmic protein in band 3 Neapolis patient without membrane association, while it was associated with the membrane in control red cells (Fig. 4; see also Fig. 4S). These data indicate that the first 11-amino acid peptide of N-terminal band 3 is critical for binding of PRDX2 to intact red cell membranes.

DISCUSSION

In the present study using multiple methodological approaches we documented that in red cells PRDX2 binds to the N-terminal cytoplasmic domain of band 3 (cdb3), and that the first 11 amino acid of the N-terminal domain of band 3 are critical for its membrane association in intact erythrocytes. PRDX2, a typical 2-Cys peroxiredoxin whose catalytic activity is responsible for detoxification of peroxides, is essential especially under oxidative stress conditions to protect cells against oxidant damage [40]. In red cells, PRDX2 is present at high copy number [4] and while it is mainly a cytosolic protein, about 5% of PRDX2 is membrane bound under normal conditions [4, 18]. Here, we showed that in response to oxidative stress there is increased membrane association of PRDX2, which is highly dependent on the availability of its docking site on the membrane. In fact, we observed different behaviour of PRDX2 membrane binding in red cells treated with either diamide, a cysteine-reacting oxidant, or PHZ, that generates free radical species acting on hemoglobin with production of hemichromes that bind to the membrane. The requirement of available membrane docking site for PRDX2 membrane association is further supported by the evidence that while PRDX2 did not bind to membrane of intact red cells treated with PHZ, with membrane associated hemichromes, it did bind to red cell membrane were oxidized with PHZ in the absence of hemoglobin and no hemichrome formation. This finding suggests that hemichromes and PRDX2 share a common binding site in agreement with our previous study showing competition between PRDX2 and hemichromes in

red cells from mouse model of β- thalassemia [18]. The docking site for hemichromes has been reported to be the N-terminal cytoplasmic domain of band 3 (cdb3) [28]. In the present study, we showed that PRDX2 binds to cdb3 with a Kd of 34 nM, indicative of high affinity interaction. SPR studies enabled us to show that the high affinity of interaction is due to a very slow off rate of the bound protein.

Previous reports have shown that deoxyhemoglobin binds a synthetic peptide of cdb3 containing the first 11 amino acids with a Kd of 0.3 mM at pH 7.2 [41], an affinity value 10^4 lower than its binding to PRDX2. Whereas, the cdb3 forms a sticky complex with hemichromes, with an affinity presumed to be much higher than that for hemoglobin, even if no structural basis for this interaction has been well established [28, 31]. The finding of increased membrane association of PRDX2 upon deoxygenation suggests that PRDX2 and deoxygenated hemoglobin binding do not share common binding sites. In this regard, N-terminal 12-23 amino acidic stretch of cdb3 has been implicated as binding site for deoxyhemoglobin although no direct Kd value for binding has been reported [31]. To evaluate whether modulation of tyrosine phosphorylation state of N-terminal domain of band 3 might affect PRDX2 membrane association similarly to that reported for glycolytic enzymes [42], we evaluated PRDX2 membrane binding in Na-vanadate treated red cells. PRDX2 similarly binds to either Na-vanadate treated red cells showing increased tyrosine phosphorylation of Tyr 8 or tyrosine phosphorylated purified cytoplasmic domain of band 3. These data suggest that changes in tyrosine phosphorylation state of N-terminal of band 3 seem not to affect PRDX2 membrane binding, as also corroborated by the similar Kd value measured in the presence of phosphorylated and unphosphorylated cytoplasmic domain of band 3.

We also have been able to document small conformational changes in PRDX2 following its binding cdb3 using spectroscopic approaches. This might be related to co-polymer formation or to minor rearrangements as have been reported for ankyrin [43, 44] or for hemoglobin [45] following their binding to cdb3. The fact that the complex cdb3-PRDX2 was protected from trypsin digestion also lends support to binding induced conformational changes. It is of interest to note that the peroxidase activity of PRDX2 was fully conserved in the complex, suggesting the two catalytic cysteine residues of each PRDX2 (Cys-51 and Cys-172) dimer (the functional active unit) are reduced and fully functional in the complex.

The stoichiometry of the interaction between cdb3 and PRDX2 is 1 cdb3 dimer with 5 PRDX2 dimers, this is reminiscent of the stoichiometry already reported for the binding of hemichromes to cdb3 [28]. Notably, the solved structure of erythrocyte PRDX2 is a decamer [6] and it is

accepted that the functionally active enzyme is the reduced decamer [6]. On the other hand, the quaternary arrangement of cdb3 is mainly dimeric or tetrameric [32, 46].

We also explored for the structural motif responsible for PRDX2 binding to cdb3. Based on the findings from studies of pH dependence of binding interactions (lower affinity at pH 8.5 and formation of co-polymers at pH 6.4) and on interaction stoichiometry (cdb3 dimer versus PRDX2 decamer), we focused our attention to the acidic N-terminal stretch of cdb3, involved in interactions with various proteins [33-39]. An analysis of the electrostatic surface potential of decameric PRDX2 showed that the interior of the toroid structure is endowed with a marked basic character (Fig. 3B). Inside the PRDX2 ring, the first residues of the N-terminal part of cdb3 could be stabilized by electrostatic interactions since it is highly acid. This could explain the higher Kd value measured at pH 8.5 that would lead to a lesser basic character of the interior of the PRDX2 decamer. The evidence that PRDX2 did not indeed associate to the membrane in the red cells from Band 3 Neapolis patient, with a truncated isoform of band-3 lacking the N-terminal 11 amino acid residues [14] supports the hypothesis that the first 11 amino acids of band-3 are essential for PRDX2 membrane association. In a previous study, Rocha et al. [47] have shown different degrees of PRDX2 membrane association in patients with hereditary spherocytosis (HS) due to various red cell membrane -protein defects. While these findings are somewhat consistant with our findings, since only 30% of patients with HS have band 3 deficiency and Rocha et al. [47] did not identify the molecular basis for HS in their patients it is difficult to directly compare their findings to ours.

In summary, we showed that cdb3 is a major docking site for PRDX2 in the red cell membrane and the first 11 amino acid of N-terminal domain of band 3 are crucial for PRDX2 membrane binding in human red cells. We suggest that the membrane association of PRDX2 with cdb3 may be important in protecting band 3 from oxidative damage and its associated membrane proteins. Further studies should be carried out to further characterize PRDX2 homeostasis in normal and diseased red cells.

ACKNOWLEDGMENTS

This work was supported by grants from FUR2010-2011, University of Verona to MB and LDF, PRIN 2008 to LDF and from Ministero Istruzione Università e Ricerca, Istituto Superiore di Sanità (AIDS Project), and CARIPLO (grant 2008-2198) to MR.

LIST OF ABBREVIATIONS

RBC: red blood cells; PRDX2: peroxiredoxin 2; PHZ: phenylhydrazine; $NaVO_3$:sodium vanadate; Hb: hemoglobin; cdb3: cytoplasmic domain band 3; SPR: real time surface plasmon resonance.

REFERENCES

[1] Mohandas, N.; Gallagher, P. G. Red cell membrane: past, present, and future. *Blood* **112:**3939-3948; 2008.

[2] Lewis, I. A.; Campanella, M. E.; Markley, J. L.; Low, P. S. Role of band 3 in regulating metabolic flux of red blood cells. *Proc Natl Acad Sci U S A* **106:**18515-18520; 2009.

[3] Campanella, M. E.; Chu, H.; Low, P. S. Assembly and regulation of a glycolytic enzyme complex on the human erythrocyte membrane. *Proc Natl Acad Sci U S A* **102:**2402-2407; 2005.

[4] Low, F. M.; Hampton, M. B.; Peskin, A. V.; Winterbourn, C. C. Peroxiredoxin 2 functions as a noncatalytic scavenger of low-level hydrogen peroxide in the erythrocyte. *Blood* **109:**2611-2617; 2007.

[5] Low, F. M.; Hampton, M. B.; Winterbourn, C. C. Peroxiredoxin 2 and peroxide metabolism in the erythrocyte. *Antioxid Redox Signal* **10:**1621-1630; 2008.

[6] Schroder, E.; Littlechild, J. A.; Lebedev, A. A.; Errington, N.; Vagin, A. A.; Isupov, M. N. Crystal structure of decameric 2-Cys peroxiredoxin from human erythrocytes at 1.7 A resolution. *Structure* **8:**605-615; 2000.

[7] Wood, Z. A.; Schroder, E.; Robin Harris, J.; Poole, L. B. Structure, mechanism and regulation of peroxiredoxins. *Trends Biochem Sci* **28:**32-40; 2003.

[8] Plishker, G. A.; Chevalier, D.; Seinsoth, L.; Moore, R. B. Calcium-activated potassium transport and high molecular weight forms of calpromotin. *J Biol Chem* **267:**21839-21843; 1992.

[9] Moore, R. B.; Shriver, S. K. Protein 7.2b of human erythrocyte membranes binds to calpromotin. *Biochem Biophys Res Commun* **232:**294-297; 1997.

[10] Moore, R. B.; Shriver, S. K.; Jenkins, L. D.; Mankad, V. N.; Shah, A. K.; Plishker, G. A. Calpromotin, a cytoplasmic protein, is associated with the formation of dense cells in sickle cell anemia. *Am J Hematol* **56:**100-106; 1997.

[11] Moore, R. B.; Mankad, M. V.; Shriver, S. K.; Mankad, V. N.; Plishker, G. A. Reconstitution of Ca(2+)-dependent K+ transport in erythrocyte membrane vesicles requires a cytoplasmic protein. *J Biol Chem* **266:**18964-18968; 1991.

[12] Biondani, A.; Turrini, F.; Carta, F.; Matte, A.; Filippini, A.; Siciliano, A.; Beuzard, Y.; De Franceschi, L. Heat-shock protein-27, -70 and peroxiredoxin-II show molecular chaperone function in sickle red cells: Evidence from transgenic sickle cell mouse model. *Proteomics Clin Appl* **2:**706-719; 2008.

[13] Moore, R. B.; Plishker, G. A.; Shriver, S. K. Purification and measurement of calpromotin, the cytoplasmic protein which activates calcium-dependent potassium transport. *Biochem Biophys Res Commun* **166:**146-153; 1990.

[14] Perrotta, S.; Borriello, A.; Scaloni, A.; De Franceschi, L.; Brunati, A. M.; Turrini, F.; Nigro, V.; del Giudice, E. M.; Nobili, B.; Conte, M. L.; Rossi, F.; Iolascon, A.; Donella-Deana, A.; Zappia, V.; Poggi, V.; Anong, W.; Low, P.; Mohandas, N.; Della Ragione, F. The N-terminal 11 amino acids of human erythrocyte band 3 are critical for aldolase binding and protein phosphorylation: implications for band 3 function. *Blood* **106:**4359-4366; 2005.

[15] Bennekou, P.; de Franceschi, L.; Pedersen, O.; Lian, L.; Asakura, T.; Evans, G.; Brugnara, C.; Christophersen, P. Treatment with NS3623, a novel Cl-conductance blocker, ameliorates erythrocyte dehydration in transgenic SAD mice: a possible new therapeutic approach for sickle cell disease. *Blood* **97:**1451-1457; 2001.

[16] Brugnara, C.; De Franceschi, L.; Alper, S. L. Ca(2+)-activated K+ transport in erythrocytes. Comparison of binding and transport inhibition by scorpion toxins. *J Biol Chem* **268:**8760-8768; 1993.

[17] Biondani A, C. F., Mattè A, Filippini A, Siciliano A, Beuzard Y, De Franceschi L. Heat-shock protein-27,-70 and peroxiredoxin-II show molecular chaperone function in sickle red cells: Evidence from transgenic sickle cell mouse model. . *PROTEOMICS CLINICAL APPLICATIONS* **2:**706-719; 2008.

[18] Matte, A.; Low, P. S.; Turrini, F.; Bertoldi, M.; Campanella, M. E.; Spano, D.; Pantaleo, A.; Siciliano, A.; De Franceschi, L. Peroxiredoxin-2 expression is increased in beta-thalassemic mouse red cells but is displaced from the membrane as a marker of oxidative stress. *Free Radic Biol Med* **49:**457-466; 2010.

[19] De Franceschi, L.; Biondani, A.; Carta, F.; Turrini, F.; Laudanna, C.; Deana, R.; Brunati, A. M.; Turretta, L.; Iolascon, A.; Perrotta, S.; Elson, A.; Bulato, C.; Brugnara, C. PTPepsilon has a critical role in signaling transduction pathways and phosphoprotein network topology in red cells. *Proteomics* **8:**4695-4708; 2008.

[20] Su, W.; Shmukler, B. E.; Chernova, M. N.; Stuart-Tilley, A. K.; de Franceschi, L.; Brugnara, C.; Alper, S. L. Mouse K-Cl cotransporter KCC1: cloning, mapping, pathological expression, and functional regulation. *The American journal of physiology* **277:**C899-912; 1999.

[21] De Franceschi, L.; Tomelleri, C.; Matte, A.; Brunati, A. M.; Bovee-Geurts, P. H.; Bertoldi, M.; Lasonder, E.; Tibaldi, E.; Danek, A.; Walker, R. H.; Jung, H. H.; Bader, B.; Siciliano, A.; Ferru, E.; Mohandas, N.; Bosman, G. J. Erythrocyte membrane changes of chorea-acanthocytosis are the result of altered Lyn kinase activity. *Blood* **118:**5652-5663; 2011.

[22] Olivieri, O.; De Franceschi, L.; Capellini, M. D.; Girelli, D.; Corrocher, R.; Brugnara, C. Oxidative damage and erythrocyte membrane transport abnormalities in thalassemias. *Blood* **84:**315-320; 1994.

[23] Anong, W. A.; Franco, T.; Chu, H.; Weis, T. L.; Devlin, E. E.; Bodine, D. M.; An, X.; Mohandas, N.; Low, P. S. Adducin forms a bridge between the erythrocyte membrane and its cytoskeleton and regulates membrane cohesion. *Blood* **114:**1904-1912; 2009.

[24] Brunati, A. M.; Bordin, L.; Clari, G.; Moret, V. The Lyn-catalyzed Tyr phosphorylation of the transmembrane band-3 protein of human erythrocytes. *Eur J Biochem* **240:**394-399; 1996.

[25] De Franceschi, L.; Bertoldi, M.; De Falco, L.; Santos Franco, S.; Ronzoni, L.; Turrini, F.; Colancecco, A.; Camaschella, C.; Cappellini, M. D.; Iolascon, A. Oxidative stress modulates heme synthesis and induces peroxiredoxin-2 as a novel cytoprotective response in beta-thalassemic erythropoiesis. *Haematologica* **96:**1595-1604; 2011.

[26] Khalifa, M. B.; Choulier, L.; Lortat-Jacob, H.; Altschuh, D.; Vernet, T. BIACORE data processing: an evaluation of the global fitting procedure. *Anal Biochem* **293:**194-203; 2001.

[27] Baker, N. A.; Sept, D.; Joseph, S.; Holst, M. J.; McCammon, J. A. Electrostatics of nanosystems: application to microtubules and the ribosome. *Proc Natl Acad Sci U S A* **98:**10037-10041; 2001.

[28] Waugh, S. M.; Low, P. S. Hemichrome binding to band 3: nucleation of Heinz bodies on the erythrocyte membrane. *Biochemistry* **24:**34-39; 1985.

[29] Pantaleo, A.; Ferru, E.; Giribaldi, G.; Mannu, F.; Carta, F.; Matte, A.; de Franceschi, L.; Turrini, F. Oxidized and poorly glycosylated band 3 is selectively phosphorylated by Syk kinase to form large membrane clusters in normal and G6PD-deficient red blood cells. *Biochem J* **418:**359-367; 2009.

[30] De Franceschi, L.; Tomelleri, C.; Matte, A.; Brunati, A. M.; Bovee-Geurts, P. H.; Bertoldi, M.; Lasonder, E.; Tibaldi, E.; Danek, A.; Walker, R. H.; Jung, H. H.; Bader, B.; Siciliano, A.; Ferru, E.; Mohandas, N.; Bosman, G. J. Erythrocyte membrane changes of chorea-acanthocytosis are the result of altered Lyn kinase activity. *Blood* **118:**5652-5663.

[31] Chu, H.; Breite, A.; Ciraolo, P.; Franco, R. S.; Low, P. S. Characterization of the deoxyhemoglobin binding site on human erythrocyte band 3: implications for O2 regulation of erythrocyte properties. *Blood* **111:**932-938; 2008.

[32] Zhang, D.; Kiyatkin, A.; Bolin, J. T.; Low, P. S. Crystallographic structure and functional interpretation of the cytoplasmic domain of erythrocyte membrane band 3. *Blood* **96:**2925-2933; 2000.

[33] Low, P. S. Structure and function of the cytoplasmic domain of band 3: center of erythrocyte membrane-peripheral protein interactions. *Biochim Biophys Acta* **864:**145-167; 1986.

[34] Cohen, C. M.; Dotimas, E.; Korsgren, C. Human erythrocyte membrane protein band 4.2 (pallidin). *Semin Hematol* **30:**119-137; 1993.

[35] Rybicki, A. C.; Schwartz, R. S.; Hustedt, E. J.; Cobb, C. E. Increased rotational mobility and extractability of band 3 from protein 4.2-deficient erythrocyte membranes: evidence of a role for protein 4.2 in strengthening the band 3-cytoskeleton linkage. *Blood* **88:**2745-2753; 1996.

[36] An, X. L.; Takakuwa, Y.; Nunomura, W.; Manno, S.; Mohandas, N. Modulation of band 3-ankyrin interaction by protein 4.1. Functional implications in regulation of erythrocyte membrane mechanical properties. *J Biol Chem* **271:**33187-33191; 1996.

[37] Rogalski, A. A.; Steck, T. L.; Waseem, A. Association of glyceraldehyde-3-phosphate dehydrogenase with the plasma membrane of the intact human red blood cell. *J Biol Chem* **264:**6438-6446; 1989.

[38] Salhany, J. M.; Cassoly, R. Kinetics of p-mercuribenzoate binding to sulfhydryl groups on the isolated cytoplasmic fragment of band 3 protein. Effect of hemoglobin binding on the conformation. *J Biol Chem* **264:**1399-1404; 1989.

[39] Harrison, M. L.; Isaacson, C. C.; Burg, D. L.; Geahlen, R. L.; Low, P. S. Phosphorylation of human erythrocyte band 3 by endogenous p72syk. *J Biol Chem* **269:**955-959; 1994.

[40] Hall, A.; Karplus, P. A.; Poole, L. B. Typical 2-Cys peroxiredoxins--structures, mechanisms and functions. *FEBS J* **276:**2469-2477; 2009.

[41] Walder, J. A.; Chatterjee, R.; Steck, T. L.; Low, P. S.; Musso, G. F.; Kaiser, E. T.; Rogers, P. H.; Arnone, A. The interaction of hemoglobin with the cytoplasmic domain of band 3 of the human erythrocyte membrane. *J Biol Chem* **259:**10238-10246; 1984.

[42] Chu, H.; Low, P. S. Mapping of glycolytic enzyme-binding sites on human erythrocyte band 3. *Biochem J* **400:**143-151; 2006.

[43] Thevenin, B. J.; Low, P. S. Kinetics and regulation of the ankyrin-band 3 interaction of the human red blood cell membrane. *J Biol Chem* **265:**16166-16172; 1990.

[44] Low, P. S.; Willardson, B. M.; Mohandas, N.; Rossi, M.; Shohet, S. Contribution of the band 3-ankyrin interaction to erythrocyte membrane mechanical stability. *Blood* **77:**1581-1586; 1991.

[45] Salhany, J. M.; Cordes, K. A.; Sloan, R. L. Characterization of the pH dependence of hemoglobin binding to band 3. Evidence for a pH-dependent conformational change within the hemoglobin-band 3 complex. *Biochim Biophys Acta* **1371:**107-113; 1998.

[46] Zhou, Z.; DeSensi, S. C.; Stein, R. A.; Brandon, S.; Dixit, M.; McArdle, E. J.; Warren, E. M.; Kroh, H. K.; Song, L.; Cobb, C. E.; Hustedt, E. J.; Beth, A. H. Solution structure of the cytoplasmic domain of erythrocyte membrane band 3 determined by site-directed spin labeling. *Biochemistry* **44:**15115-15128; 2005.

[47] Rocha, S.; Vitorino, R. M.; Lemos-Amado, F. M.; Castro, E. B.; Rocha-Pereira, P.; Barbot, J.; Cleto, E.; Ferreira, F.; Quintanilha, A.; Belo, L.; Santos-Silva, A. Presence of cytosolic peroxiredoxin 2 in the erythrocyte membrane of patients with hereditary spherocytosis. *Blood Cells Mol Dis* **41:**5-9; 2008.

FIGURE LEGENDS

Fig. 1. (A) Immunoblot analysis of red cell membrane with specific antibody anti-peroxiredoxin 2 (PRDX2), anti-band 3 (B3) and anti-tyrosine phosphorylated band 3 on residue 8 (B3 PY8). Actin was used as loading control. Red cells were treated with phenylhydrazine (PHZ) 100 µM or diamide 2 mM or Na_3VO_4 0.1 mM. Shown is a representative experiment of 6 performed with similar results. Tween colloidal Coomassie stained gels and densitometric analysis of the immuno-blots are shown in Supplement data (Fig. 1SA and 1SB). **(B)** Immuno-blot analysis with specific anti-PRDX2 antibody of red cell membrane treated with phenylhydrazine (PHZ) 100 µM or diamide 2 mM or Na_3VO_4 0.1 mM. Samples were run under not reducing condition, bands at 19 and 37 kDa represent PRDX2 monomers (M) and dimers (D) respectively. Actin was used as loading control. Tween colloidal Coomassie stained gels and densitometric analysis of the immuno-blots are shown in Supplement data (Fig. 1SC and 1SD). Shown is a representative experiment of 6 others performed with similar results. **(C)** Immuno-blot analysis with specific anti-PRDX2 antibody of red cell membrane from native red cells (control), red cells exposed to phenylhydrazine (PHZ, 100 µM) or Diamide (2 mM) or Na_3VO_4 (0.1 mM) incubated with cytoplasm fraction of control red cells containing native PRDX2. The last 2 lanes are red cell membrane treated with either phenylhydrazine (PHZ, 100 µM) or Diamide (2 mM) and incubated with either Tween colloidal Coomassie stained gels and densitometric analysis of the immuno-blots are shown in Supplement data (Fig. 2SA and 2SB). Shown is a representative experiment of 3 others performed with similar results. **(D)** Immuno-blot analysis with specific anti-PRDX2 antibody of red cell membrane from red cells under oxygenation (Oxy) and deoxygenation (Deoxy) condition (see details in Material and Methods). Actin was used as loading control. Shown is a representative experiment of 3 others performed with similar results. Densitometric analysis of the immuno-blots are shown in Supplement data Fig. 2SC.

Fig. 2. (A) PRDX2 binding proteins in KI-IOVs revealed by cross-linking experiments. Recombinant PRDX2 (0.5 mg/ml) was incubated in the dark with 5-fold molar excess of sulfo-SBED for 30 minutes at room temperature. Thereafter, the protein solution was extensively

dialyzed overnight against PBS to remove excess sulfo-SBED. The labeled PRDX2 was then recovered, aliquoted and kept at -80°C. KI-IOVs (100 μg) were incubated with 5 μg of PRDX2-sulfo-SBED for 1 hour at room temperature in the dark to allow membrane association, after which cross-linking to nearest neighbor proteins was activated by exposure for 15 min to a UV 366 nm light source at a distance of 5-10 cm. A total of 100 mM DTT was then added to reduce the disulfide linkage between sulfo-SBED-PRDX2 and its membrane targets. The samples were separated by mono-dmensional electrophoresis and blotted for streptavidin-horseradish peroxidase detection. Colloidal Comassie stained gel: molecular wight standard (marker: M); lane 1 recombinant PRDX2; lane 2; PRDX2 and KI-IOV; lane 3: KI-IOV. Blots (Sulfo-SBED): lane 1 recombinant PRDX2; lane 2; PRDX2 and KI-IOV; lane 3: KI-IOV. Western-blot (Wb) analysis with specific anti band 3 antibody: lane 1 recombinant PRDX2; lane 2; PRDX2 and KI-IOV; lane 3: KI-IOV. The membrane used for streptavidin-horseradish peroxidase blots were incubated with specifict anti-band 3 antibody and anti-α-, β- spectrin antibody. Shown is a representative experiment of 4 others performed with similar results. The asterix indicated the proteins identified by mass spectrometric analysis (from top to bottom): Ankyrin repeated domain-containing protein 40 (Q6AI12), 12% coverage; Band 3 anion transport protein (P02730) 9% coverage; Band 4.2 (P16452) 15 % coverage; Stomatin (P27105) 29% coverage.

(B) Binding of PRDX2 to cdb3 by intrinsic fluorescence measurements. PRDX2 (4 μM) was reacted with different concentrations of cdb3 (10-180 nM) in 50 mM Hepes pH 7.4 or 50 mM sodium phosphate buffer, 0.1 M NaCl, pH 7.4, at 25°C. After reaching equilibrium (15-20 min) the emission spectrum was recorded upon excitation at 295 nm. The dotted line refers to PRDX2 alone, while the straight lines refer to spectra of PRDX2 following increasing concentrations of cdbs (from top to bottom). Inset: The difference in the maximum fluorescence emission centered at 338 nm plotted versus cdb3 concentration follows an hyperbolic behaviour which was fit to equation 1 to obtain the equilibrium dissociation constant, Kd.

(C) SPR analysis of PRDX2/Cdb3 interaction. Upper panel: Sensorgrams showing the binding of PRDX2 (900 nM) to a BIAcore sensorchip coated with Cdb3- or with an anti-N-terminal band 3 antibody. **Lower panel:** Blank-subtracted sensorgram overlay showing the binding of increasing concentrations of PRDX2 (1,250, 1,000, 900, 800, 650, 300 nM) to a Cdb3-coated BIAcore sensorchip. In both the panels, the response (in resonance units, RU) was recorded as a function of time.

(D) Near UV circular dichroism spectra of PRDX2 in the presence of cdb3. PRDX2 (20 μM, 0.44 mg/ml) was incubated in the presence of saturating cdb3 concentration (2.3 mM, 0.1 mg/ml) and spectra were recorded during the time of CD spectral changes without averaging. The dotted line refers to PRDX2 alone, while the straight lines refer to spectra of PRDX2 in the presence of cdb3 at the indicated times.

Fig. 3. (A) Molecular surface analysis of PRDX2. The relative electrostatic potentials are indicated by the following colours: regions negatively or positively charged are represented in red or blues, respectively. The white colour shows the region without charge **(B) Determination of PRDX2-cdb3 stoichiometry.** PRDX2, 1 μl of a 10 mg/ml solution, in 50 mM Hepes pH 6.4 (10 μg total) was added to two different solutions of cdb3: mixture 1 containing 20 μl of a 0.25 mg/ml solution (5 μg total) and mixture 2 containing 40 μl of a 0.25 mg/ml solution (10 μg total). After 15 minutes incubation, the mixtures were centrifuged, and the supernatants were separated from pellets. 12 μl of each supernatant was treated with 4 μl of SDS sample buffer 4X, while the pellets were solubilized with 12 μl of SDS Sample buffer 1X. After one hour incubation, all samples were loaded onto SDS-PAGE. The gel shown contains: lane 1: 10 μg PRDX2 control, lane 2: 5 μg cdb3 control, lane 3: supernatant reaction mixture 1 (S1), lane 4: supernatant reaction mixture 2 (S2), lane 5: pellet reaction mixture 1 (P1) and lane 6: pellet reaction mixture 2 (P2).

Fig. 4. (A) Immuno-blot analysis with specific anti- peroxiredoxin 2 (PRDX2) antibody of red blood cell (RBC) membrane (ghost), RBC cytosol fraction and total RBC lysates from control and B3 Neapolis patient. Shown is a representative experiment of 3 others performed with similar results. **(B)** Immunofluorescence staining with anti-PRDX2 antibody and corresponding brightfield images of fixed and permeabilized red cells from control and B3 Neapolis patient. Shown is a representative experiment of 4 performed with similar results (see also supplement Fig. 5S for secondary antibody controls).

TABLE 1. Binding parameters of the interaction of PRDX2 with Cdb3 immobilized to a BIAcore sensorchip.

	k_{on} (M^{-1} s^{-1})	k_{off} (s^{-1})	Kd (M) (k_{on}/k_{off})
PRDX2	1.48×10^{2}	9.76×10^{-6}	6.61×10^{-8}
anti-cdb3 antibody	3.61×10^{5}	6.78×10^{-4}	1.88×10^{-9}

A specific anti-cdb3 antibody was used as a positive binding control for cdb3. k_{on} and k_{off} are reported. K_d value was derived from the k_{off}/k_{on} ratio. The results shown are representative of other two that gave similar results. Only sensorgrams whose fitting gave values of *x*2 close to 10 were used [26].

SUPPLEMENTAL FIGURES LEGENDS

Fig. 1S. (A) Tween colloidal Coomassie stained gels of Fig. 1A immuno-blot analysis with specific anti-Prx2 antibody of red cell membrane (ghost) (b) from red cells (control) without and with phenylhydrazine (PHZ, 100 µM), Diamide (2 mM) or Na_3VO_4 (0.1 mM) treatment. Shown is a representative experiment of 6 others performed with similar results. **(B)** Relative quantification of immunoreactivity of Prx2 and band 3 phosphorylated on Tyr-8 associated to the red cell membrane from red cells (control) without and with phenylhydrazine (PHZ, 100 µM), Diamide (2 mM) or Na_3VO_4 (0.1 mM) treatment (see Fig. 1A). Data are presented as means ±SD (*n*=6); **P*<0.05 compared to untreated red cells **(C)** Tween colloidal Coomassie stained gels of Fig. 1A immuno-blot analysis with specific anti-Prx2 antibody of red cell membrane (ghost) from red cells (control) without and with phenylhydrazine (PHZ, 100 µM), Diamide (2 mM) or Na_3VO_4 (0.1 mM) treatment. Shown is a representative experiment of 6 others performed with similar results. **(D)** Relative quantification of immunoreactivity of Prx2 associated to the red cell membrane from red cells (control) without and with phenylhydrazine (PHZ, 100 µM), Diamide (2 mM) or Na_3VO_4 (0.1 mM) treatment (see Fig. 1B). Data are presented as means ±SD (*n*=6); **P*<0.05 compared to untreated red cells. **(E)** Heme amounts in red cell membranes untreated or treated with PHZ or diamide. Red cell membranes were treated as reported in the Material and Methods Section. Heme concentrations were evaluated as reported

in Supplemental Material and Methods section. Experiments were repeated in triplicate, here the mean and the S.E.M. is reported.

Fig. 2S. (A) Tween colloidal Coomassie stained gels of Fig. 1C immunoblot analysis with specific anti-Prx2 antibody of red cell membrane from control red cells and red cells exposed to phenylhydrazine (PHZ, 100 μM), Diamide (2 mM) or Na_3VO_4 (0.1 mM); isolated red cell membranes treated with PHZ (50 μM,) diamide (2 mM) incubated with cytoplasm fraction of untreated red cells. Shown is a representative experiment of 3 others performed with similar results. **(B)** Relative quantification of immunoreactivity of Prx2 associated to the red cell membrane of control red cells and red cells exposed to phenylhydrazine (PHZ, 100 μM), Diamide (2 mM) or Na_3VO_4 (0.1 mM); isolated red cell membranes treated with PHZ (50 μM,) diamide (2 mM) incubated with cytoplasm fraction of untreated red cells (see Fig. 1C). Data are presented as means ±SD (*n*=6); **P*<0.05 compared to controls. **(C)** Relative quantification of immunoreactivity of Prx2 associated to the red cell membrane from red cells exposed to oxygenation and deoxygenation, see Fig. 1D. Data are presented as means ±SD (*n*=3); **P*<0.05 compared to oxygenated red cells.

(D-E) Proteolytic cleavage of PRDX2 in the absence (C) or presence (D) of cdb3. (D) PRDX2 (0.5 mg/ml) was treated with trypsin (1:50, w:w). At the indicated times, aliquots were withdrawn, boiled and loaded onto SDS-PAGE. **(E)** Cdb3 (0.1 mg/ml) was added to PRDX2 (0.4 mg/ml) followed by 20-min incubation. The mixture was then treated with trypsin (1:50, w:w). At the indicated times, aliquots were withdrawn, boiled and loaded onto SDS-PAGE.

Fig. 3S. Binding of PRDX2 to cdb3 by intrinsic fluorescence measurements. PRDX2 (4 μM) was reacted with different concentrations of cdb3 (10-180 nM) in 50 mM Hepes pH 8.4 at 25°C. After reaching equilibrium (15-20 min) the emission spectrum was recorded upon excitation at 295 nm. The dotted line refers to PRDX2 alone, while the straight lines refer to spectra of PRDX2 following increasing concentrations of cdb (from top to bottom). Inset: The difference in the maximum fluorescence emission centered at 338 nm plotted versus cdb3 concentration follows an hyperbolic behaviour which was fit to equation 1 to obtain the equilibrium dissociation constant, Kd.

Fig. 4S. Electrostatic surface potential calculation of dimeric PRDX2 and the 11 amino acid N-terminal domain of band 3. The relative electrostatic potentials are indicated by the following colours: regions negatively or positively charged are represented in red or blues, respectively. The white colour shows the region without charge. (**A)** Dimeric PRDX2 showing

the monomer-monomer interaction crevice. (**B)** Dimeric PRDX2 on the opposite side facing the hole of the center of the ring in the decamer assemblage. (**C)** The highly anionic 11 amino acid N-terminal peptide of band 3.

Fig. 5S. Confocal immunofluorescence using secondary antibody control (rabbit IgG isotypic control and Alexa Fluor 594 goat anti-rabbit IgG) images of fixed and permeabilized red cells from control and Band 3 Neapolis patient.

HIGHLIGHTS

- The cytoplasmic domain of B3 is the docking site for PRDX2
- Binding of PRDX2 to the cytoplasmic domain of B3 determines a conformational change
- The complex PRDX2-cytoplasmic domain of B3 exhibits peroxidase activity
- The first 11 aa of B3 cytoplasmic domain are important for PRDX2 binding

Figure 1

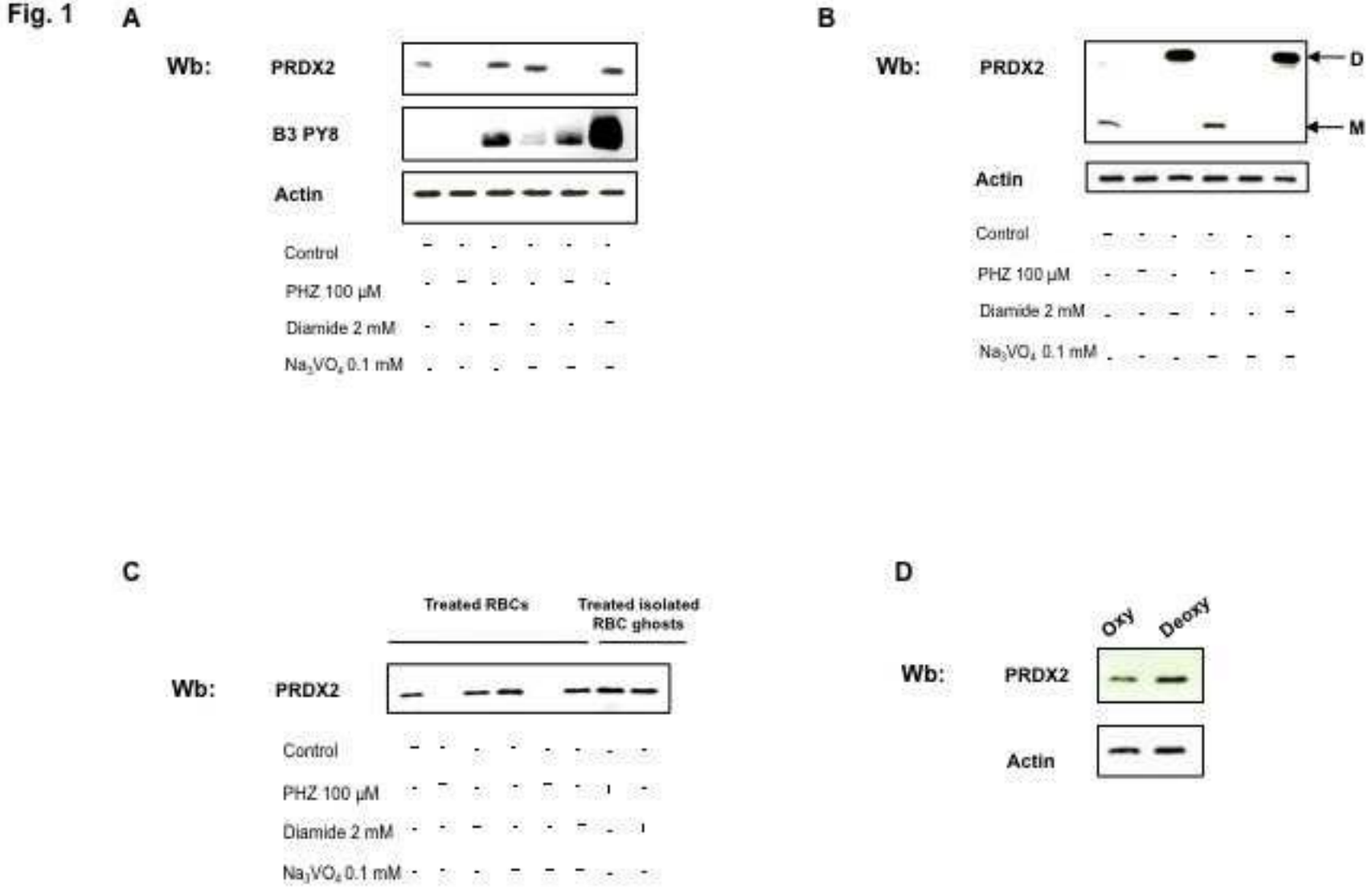

Figure 2

Fig. 2

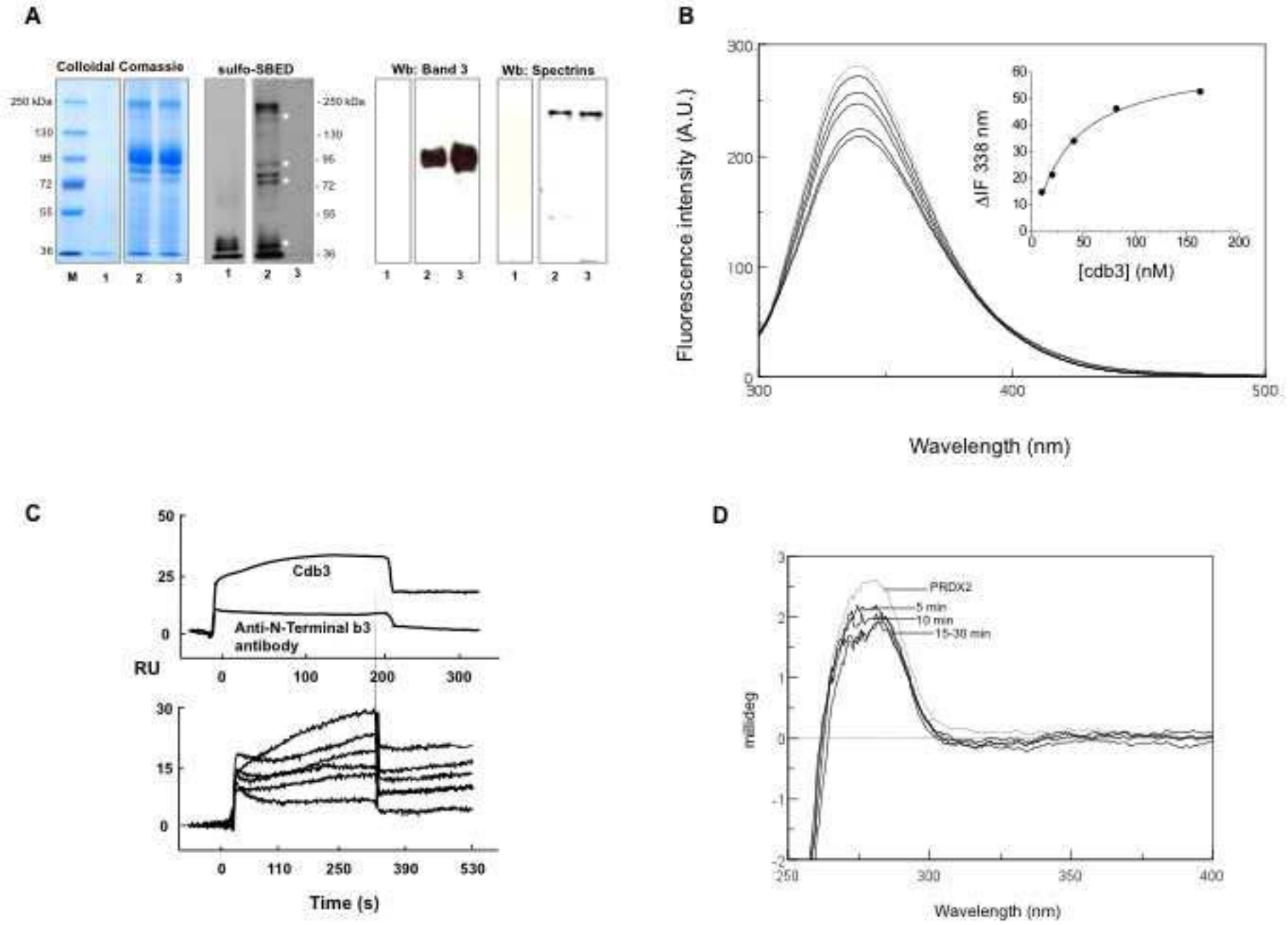

Figure 3

Fig. 3

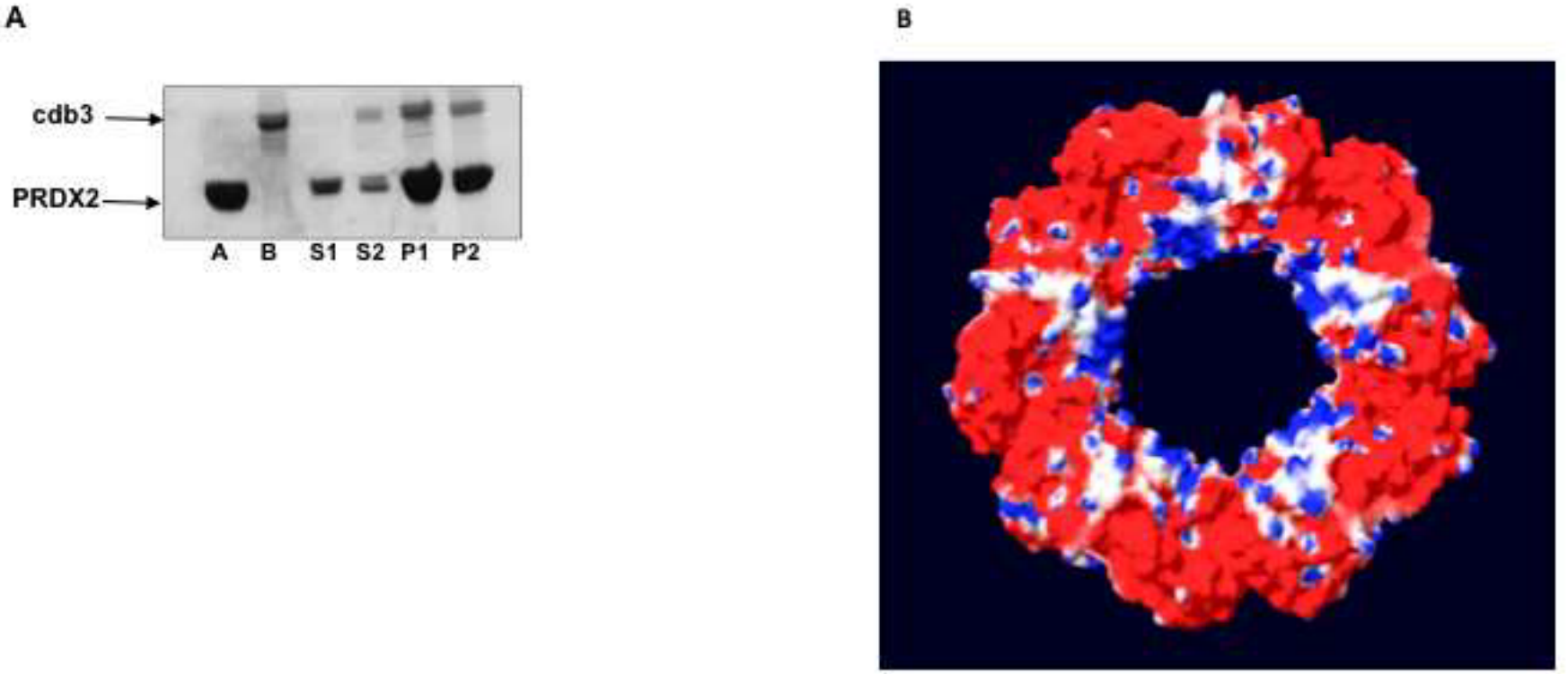

Figure(s)

Fig. 4